International Journal of Engineering, Mathematical and Physical Sciences
ISSN: 2517-9934
Vol:1, No:11, 2007

2D Fracture Analysis of the First Compression Piston Ring

I. Razmi, and N. Choupani

***Abstract*—**The incidence of mechanical fracture of an automobile piston rings prompted development of fracture analysis method on this case. The three rings (two compression rings and one oil ring) were smashed into several parts during the power-test (after manufacturing the engine) causing piston and liner to be damaged. The radial and oblique cracking happened on the failed piston rings. The aim of the fracture mechanics simulations presented in this paper was the calculation of particular effective fracture mechanics parameters, such as J-integrals and stress intensity factors. Crack propagation angles were calculated as well. Two-dimensional fracture analysis of the first compression ring has been developed in this paper using ABAQUS CAE6.5-1 software. Moreover, SEM fractography was developed on fracture surfaces and is discussed in this paper. Results of numerical calculations constitute the basis for further research on real object.

***Keywords*—**Compression piston ring, Crack, Fracture mechanics, SEM fractography.

I. Introduction

THE primary role of the piston ring pack is to maintain an effective gas seal between the combustion chamber and the crankcase. The rings of the piston ring pack, which together effectively form a labyrinth seal, achieve this by closely conforming to their grooves in the piston and to the cylinder wall. The small quantity of gas that does find its way into the crankcase, blow-by, is normally piped back to the inlet valve and fed back into the cylinder.

In addition to causing a dramatic increase in pressure, the combustion event generates a large amount of heat. Much of this thermal energy is convected into the piston causing a marked increase in the temperature of the piston, which is dissipated by heat transfer to adjacent components and the engine coolant. The secondary role of the piston ring pack is to transfer this heat from the piston into the cylinder wall and thence into the coolant.

The final function of the piston ring pack is to limit the amount of oil that is transported from the crankcase to the combustion chamber. This flow path is probably the largest contributor to the oil consumption of an engine and leads to an increase in harmful exhaust emissions as the oil mixes and reacts with the other contents of the combustion chamber [1].

Authors are with Department of Mechanical Engineering, Sahand University of Technology, P.O. Box 51335-1996, Tabriz, Iran (e-mail: i_razmi@sut.ac.ir, i_razmi@yahoo.com).

The piston ring pack must fulfil these three roles with a minimum of frictional power loss, most notably at the sliding interface with the cylinder wall, and a minimum of wear in order to maximize component life [2].

It was reported that after manufacturing the engine, the abnormal sound and vibrations sent out from engine during the power-test. The engine was disassembled and it was found that piston rings were smashed into several parts and cylinder liner, piston and connecting-rod were damaged. The paper describes two-dimensional fracture mechanics approach to the failed first compression ring and a fractographic study.

II. Mathematical Formulations

A. J-Integral in Two Dimensions

The J-integral is usually used in rate-independent quasi-static fracture analysis to characterize the energy release associated with crack growth. The J-integral is defined in terms of the energy release rate associated with crack advance. In the context of quasi−static analysis, the J-integral is defined in two dimensions as

$$J = \lim_{\Gamma \to 0} \int_{\Gamma} n.H.qd\Gamma \tag{1}$$

where Γ is a contour beginning on the bottom crack surface and ending on the top surface, as shown in Fig. 1; the limit $\Gamma \to 0$ indicates that Γ shrinks onto the crack tip; $\boldsymbol{q}$ is a unit vector in the virtual crack extension direction; and $\boldsymbol{n}$ is the outward normal to Γ. $\boldsymbol{H}$ is given by

$$\mathrm{H} = WI - \sigma.\frac{\partial u}{\partial x} \tag{2}$$

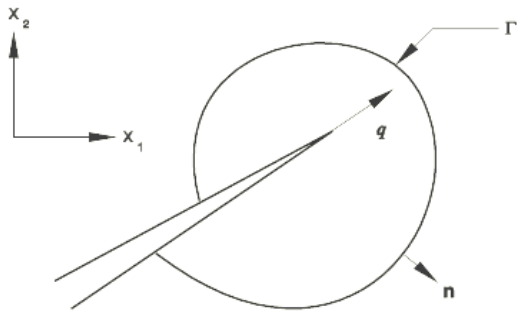

Fig. 1 Contour for evaluation of the J-integral

[3]. ***H*** is a complex stress function where ***I*** denotes the imaginary part of the function, i.e. $i = \sqrt{-1}$, σ is the loaded stress and ***u*** is the displacement [4]. For elastic material behavior ***W*** is the elastic strain energy; for elastic−plastic material behavior ***W*** is defined as the elastic strain energy density plus the plastic dissipation, thus representing the strain energy in an "equivalent elastic material". This implies that the J-integral calculation is suitable only for monotonic loading of elastic−plastic materials [3].

B. Stress Intensity Factor Extraction

The stress intensity factors $\boldsymbol{K}_{\mathrm{I}}$, $\boldsymbol{K}_{\mathrm{II}}$, and $\boldsymbol{K}_{\mathrm{III}}$ play an important role in linear elastic fracture mechanics. They characterize the influence of load or deformation on the magnitude of the crack tip stress and strain fields and measure the propensity for crack propagation or the crack driving forces. Furthermore, the stress intensity can be related to the energy release rate (the J-integral) for a linear elastic material through

$$J = \frac{1}{8\pi} K^T . B^{-1} . K \tag{3}$$

where $K = \begin{bmatrix} K_I & K_{II} & K_{III} \end{bmatrix}^T$ and ***B*** is called the pre−logarithmic energy factor matrix (Shih and Asaro, 1988; Barnett and Asaro, 1972; Gao, Abbudi, and Barnett, 1991; Suo, 1990). For homogeneous, isotropic materials ***B*** is diagonal and the above equation simplifies to

$$J = \frac{1}{\overline{E}}(K_I^2 + K_{II}^2) + \frac{1}{2G} K_{III}^2 \tag{4}$$

where $\overline{E} = E$ for plane stress and ***G*** is the torsional modulus.

For homogeneous, isotropic elastic materials the direction of cracking initiation can be calculated using one of the following three criteria: the maximum tangential stress criterion, the maximum energy release rate criterion, or the $\boldsymbol{K}_{\mathrm{II}}$ criterion. $\boldsymbol{K}_{\mathrm{III}}$ is not taken into account in any of these criteria.

1) The maximum tangential stress criterion

Using either the condition $\partial \sigma_{\theta\theta} / \partial \theta = 0$ or $\tau_{r\theta} = 0$ (where *r* and θ are polar coordinates centered at the crack tip in a plane orthogonal to the crack line), we can obtain

$$\hat{\theta} = \cos^{-1}\left(\frac{3K_{II}^2 + \sqrt{K_I^4 + 8K_I^2 K_{II}^2}}{K_I^2 + 9K_{II}^2} \right) \tag{5}$$

where the crack propagation angle $\hat{\theta}$ is measured with respect to the crack plane and $\hat{\theta} = 0$ represents the crack propagation in the "straight-ahead" direction. $\hat{\theta} < 0$ if $K_{II} > 0$ while $\hat{\theta} > 0$ if $K_{II} < 0$. The crack propagation angle is measured from ***q*** to ***n***; i.e., it is counterclockwise measured from ***q*** in Fig. 1.

2) The maximum energy release rate criterion

This criterion postulates that a crack initially propagates in the direction that maximizes the energy release rate.

3) The $\mathbf{K}_{\mathrm{II}} = 0$ criterion

This criterion assumes that a crack initially propagates in the direction that makes $\boldsymbol{K}_{II} = 0$.

The crack propagation angle $\hat{\theta}$ will be output of these criteria [3].

III. SEM Observation

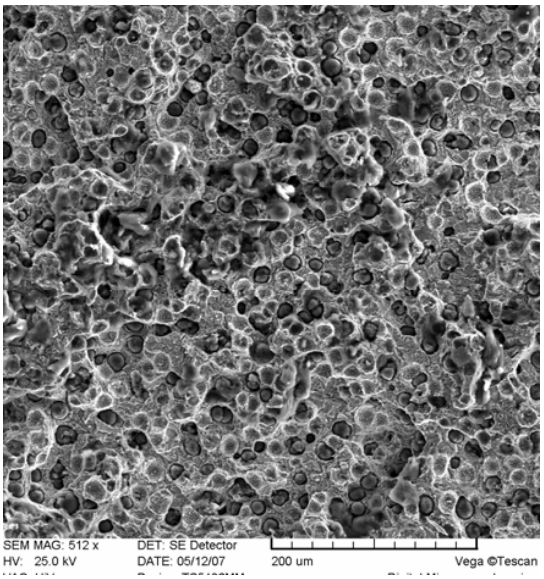

Fig. 2 SEM fractograph of the ring showing ductile fracture (512 times magnified)

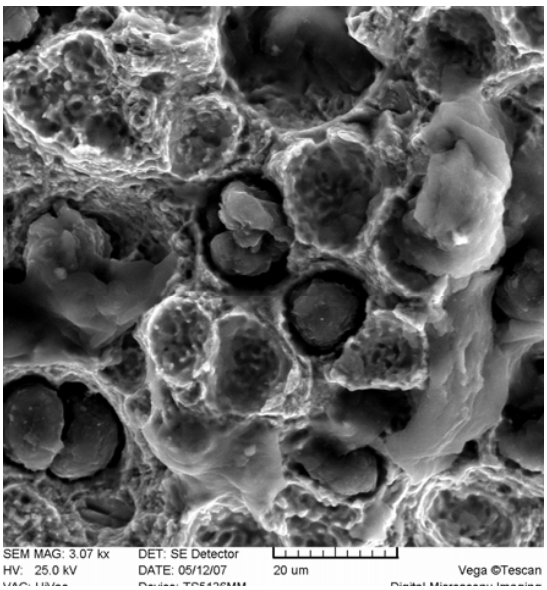

Fig. 3 Inclusions have nucleated the voids (3007 times enlarged)

Scanning electron microscope (SEM) fractography was developed on fracture surface of the ring. Fig. 2 and 3 are SEM fractographs which show dimpled fracture surfaces that are typical of microvoid coalescence. Fig. 3 shows inclusions that nucleated the voids. Apparently, ductile fracture has occurred.

IV. Fracture Mechanics Approach

The procedure consists of several steps.

A. Geometry and Model

The real ring was measured and the 2D part was formed by two concentric circles of known radii and a ring gap as shown in Fig. 4. Geometrical specifications of the 2D model are listed in Table I. A crack was embedded 180 degrees opposite to the ring gap.

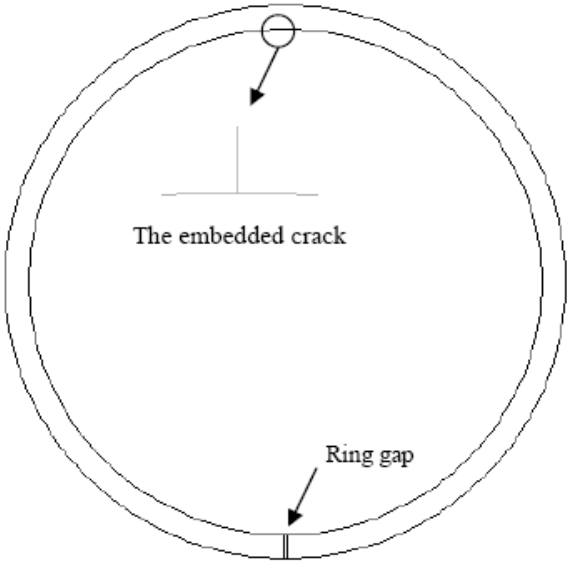

Fig. 4 2D model of the first compression ring

TABLE I
Geometrical Specifications of the 2D Model

	mm
Inner diameter	68.69
Outer diameter	74.97
Ring gap	0.3

In order to create the singularity at the crack tip to improve the accuracy of the J-integral and the stress intensity factors, the model was partitioned such that a ring of fine collapsed quadrilateral elements, as shown in Fig. 5, could be created around the crack tip.

To obtain the mesh singularity, second-order elements were used and the elements were collapsed as follows:

- One side of an 8-node isoparametric element was collapsed so that all three nodes—a, b and c—had the same geometric location (on the crack tip).
- The midside nodes on the sides connected to the crack tip was moved to the 1/4 point nearest the crack tip.

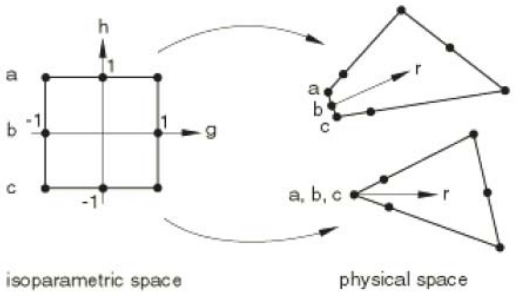

Fig. 5 Collapsed two-dimensional element

In a finite element model, each evaluation can be thought of as the virtual motion of a block of material surrounding the crack tip (in two dimensions). Each such block is defined by contours: each contour is a ring of elements completely surrounding the crack tip. These rings of elements are defined recursively to surround all previous contours. The first ring of elements that lie within the crack tip domain used for the calculations are 6-node quadratic plane stress triangles (CPS6M) and the rest are 8-node biquadratic plane stress quadrilaterals (CPS8R) as shown in Fig. 6. The element size is increased as you move away from the crack tip. The crack properties such as crack front and crack extension direction were defined. In two dimensional fracture analysis, the crack front (first contour region) is the same as the crack tip. The crack extension direction was defined starting from the crack tip and going radially towards the external circle. Each contour provides an evaluation of the contour integral. The number of evaluations possible is the number of such rings of elements. 5 contours were specified to be used in calculating contour integrals.

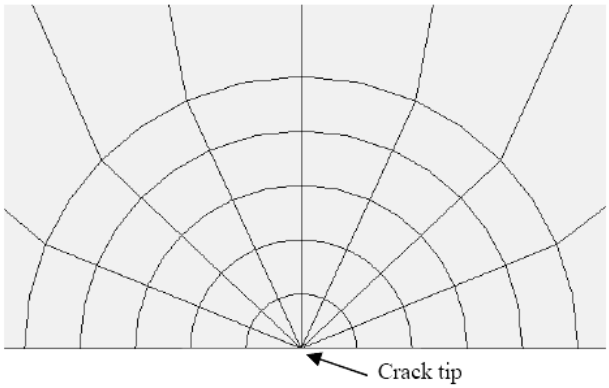

Fig. 6 6-node quadratic triangles and 8-node biquadratic quadrilaterals surrounded the crack tip

B. Material Properties

The material is assumed to be linear elastic. Piston rings operate at high temperatures and considerable varying loads. They are fabricated from cast iron or alloy cast iron. For grey cast iron, the modulus of elasticity (***E***) of the ring material is 1×10^5 Mpa [5].

C. Loading and Boundary Conditions

A static uniform circumferential pressure of 0.223 Mpa against the cylinder liner was applied to the inner part of the ring [5]. In accordance with the work conditions of the ring in a combustion engine ring seal, which consists of an assembly of piston rings, piston and cylinder liner [6], the model was restrained symmetrically from any displacement along the radial direction and any rotation along its axis.

D. The Final Compression Piston Ring Model

Except for the first five contours, the rest of the model has a coarse mesh; it was attempted to approximate the coarse meshes to square-shaped meshes. A part of the final meshed model is shown in Fig. 7. Table II shows number of finite elements in the piston ring model.

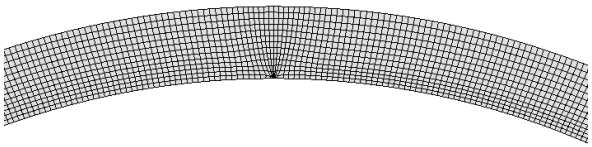

Fig. 7 A part of meshed model near the embedded crack

TABLE II
NUMBER OF FES IN THE PISTON RING MODEL

	Number of elements	Number of nodes
Piston ring	11768	37133

The final model was analyzed by ABAQUS/CAE 6.5-1 to give an estimate of J-integrals, stress intensity factors and crack propagation angles in the first 5 contours. To determine crack propagation angles, three crack initiation criteria, cited previously, were used.

V. RESULTS AND DISCUSSION

The simulation led to the desired results. J-integral estimates are shown in Table III. In linear elastic problems the first and second contours typically should be ignored as inaccurate, thus the average value of the J-integral is calculated based on contours 3, 4 and 5.

TABLE III
J-INTEGRAL ESTIMATES[A] ($\times 10^{-7}$) FOR THE CRACK[B]

Contour	J value	Average value, Contours 3-5
1	-6.0781E-03	
2	-6.0737E-03	
3	-6.2356E-03	-6.21E-03
4	-6.2436E-03	
5	-6.1597E-03	

[A] Unit is J/m^2.
[B] Contours 1 and 2 are omitted from the average value calculations.

TABLE IV
STRESS INTENSITY FACTORS[A] ESTIMATE

Contours	K_I	K_{II}
1	0.5236E-03	-0.5926E-02
2	0.5256E-03	-0.5926E-02
3	0.6903E-02	-0.5920E-02
4	0.1602E-01	-0.5917E-02
5	0.1505E-01	-0.5916E-02

[A] Unit is Mpa.m$^{1/2}$

In addition, the stress intensity factors were calculated. Since the crack front is very close to the symmetry axis, more refined meshes should be used to make the plane strain condition prevail locally around the crack front so that contour-independent results can be obtained. The calculated values of the stress intensity factors $\boldsymbol{K}_{\mathrm{I}}$ and $\boldsymbol{K}_{\mathrm{II}}$ are shown in Table IV.

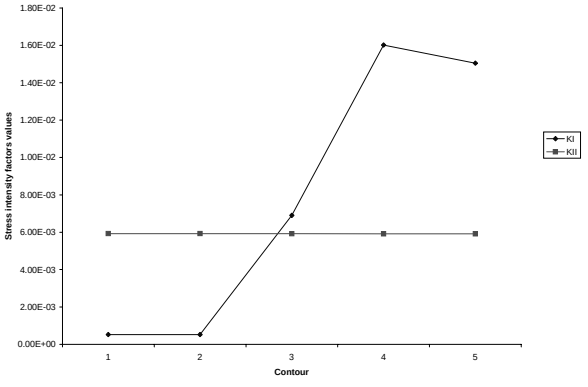

Fig. 8 Sequence of stress intensity factors estimates in the fist five contours

Fig. 8 illustrates how K_I values, corresponding to opening mode (mode-I of fracture), differ through contours; while K_{II} values which correspond to shearing mode (mode-II of fracture) remain almost steady. After K_I value remains approximately constant from contour 1 to 2, it increases significantly and reaches a peak in contour 4. Subsequently, there is a slight drop from contour 4 to 5.

Crack propagation angles are obtained based on three criteria cited previously. Results are shown in Table V. Fig. 9 shows a comparison between crack propagation angles in the first five contours.

TABLE V
CRACK PROPAGATION ANGLES[A]

Contours	Maximum tangential stress criterion	Maximum energy release rate criterion	$K_{II} = 0$ criterion
1	68.85	73.98	75.38
2	68.84	73.98	75.35
3	50.66	53.78	54.07
4	33.61	34.74	34.78
5	34.97	36.25	36.29

[A] Angles are in degree.

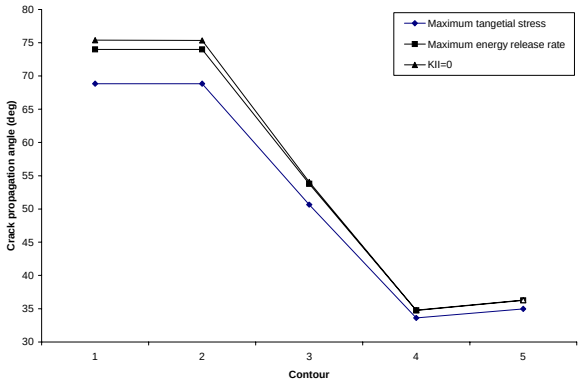

Fig. 9 Comparison between crack propagation angles in the first five contours obtained from three criteria

As it is obvious, "Maximum energy release rate" criterion and "$K_{II} = 0$" criterion are in agreement with a little difference.

Later studies shall be developed on comparing simulation estimates with experimental results.

REFERENCES

[1] S.T. Gazzard, D.R. Eastham, R.J. Jakobs, and R.L. Lunsford, "Piston system design for low emissions, Leading through Innovation", T&N Symposium, 1995, Paper 20.
[2] M. Priest, D. Dowson, and C.M. Taylor, "Predictive wear modeling of lubricated piston rings in a diesel engine", Wear 231, 1999, pp. 89–101.
[3] ABAQUS/Standard Theory Manual
[4] T.L. Anderson, *Fracture mechanics-Fundamentals and applications*. 2nd ed., CRC Press LLC, 1995, pp. 109-115.
[5] A. Kolchin, and V. Demidov, *Design of automotive engines*, Moscow, Mir Publishers, 1984, pp. 234-238.
[6] A. Kazmierczak, "Computer simulation of piston–piston ring–cylinder liner coactions in combustion engines", Proceedings of the Institution of Mechanical Engineers, 2004, pp. 1491-1501